Lithuanian Journal of Physics, Vol. **45**, No. 2, pp. 95–100 (2005) doi:10.3952/lithjphys.45204

MODELLING EFFICIENT NL-PML BOUNDARY CONDITIONS FOR THE NONPARAXIAL BEAM PROPAGATION METHOD

R. Petruškevičius

Institute of Physics, Savanorių 231, LT-02300 Vilnius, Lithuania
E-mail: raimisp@ktl.mii.lt

Received 31 January 2005

The nonlinear perfectly matched layer (NL-PML) boundary conditions were successfully applied to the nonparaxial beam propagation method. It is demonstrated that the NL-PML is extremely effective in absorbing the outgoing spatial solitons that impinge the boundary of computation domain for a wide angular spectrum of wave propagation. Using of sufficiently smooth conductivity profiles and termination of NL-PML media by controlled transparent boundary conditions offer further significant improvement in the accuracy of the numerical solutions of the nonparaxial beam propagation method at the grazing angles.

Keywords: nonparaxial beam propagation, boundary conditions, parametric spatial solitons, quasi-phase matching

PACS: 42.25.Bs, 42.65.Tg, 42.65.Yj

1. Introduction

It is of great importance to have powerful and flexible tools of analysis to simulate, design and optimize photonic circuit devices. The finite-difference time-domain (FDTD) simulation tools of optical devices and optical storage systems [1] usually suffer from inefficiency due to long computation times and requirements of large memory for storage. FDTD algorithm is suitable for modelling of wave propagation in the small volumes and for the short propagation times [2]. The beam propagation method (BPM) based on paraxial approach [3] is the most popular technique employed to investigate light propagation in integrated optical devices. The drawback of this technique is the necessity to accurately guess reference indices to satisfy slowly varying envelope approximation (SVEA) and the inability to treat reflections generated by refractive index variations. Paraxiality limitation of conventional BPM is removed by using nonparaxial, wide-angle formulation of BPM [4]. The nonparaxial BPM can simulate fields with rapidly changing envelopes and there is no need to accurately guess reference indices. This allows the simulation of multiple waves travelling at very different angles, wave mixing with large phase mismatching, wide-angle interactions and scattering in subwavelength structures of optical devices.

In implementation of nonparaxial and bidirectional BPM for simulation of open space propagation, boundary conditions play very important role, because popular technique, transparent boundary conditions (TBC) [5], have very limited effectiveness [6]. Novel boundary conditions, perfectly matched layer (PML) ones, were proposed by Bérenger [7]. The effectiveness of PML boundary conditions was subsequently verified by other groups [8, 9], also for linear [10] and nonlinear [11] nonparaxial BPM. In this paper, the investigation of effectiveness of nonlinear PML (NL-PML) boundary conditions terminated by different realisations of TBC (adaptive, controlled, and uniform TBC) is reported. NL-PML boundary conditions terminated by controlled TBC, which extremely improve the outgoing wave absorption for small tilted propagation angles, were proposed. These boundary conditions are most suitable for nonparaxial simulations.

2. Boundary conditions for the nonparaxial beam propagation method

As an example for testing of NL-PML boundary conditions for nonparaxial BPM we will consider three wave mixing process in parametric downconversion configuration [12–14] in bulk media of periodically poled lithium niobate (PPLN). We will investigate tilted propagation of pump, signal, and idler beams, with fre-

© Lithuanian Physical Society, 2005
© Lithuanian Academy of Sciences, 2005
ISSN 1648-8504

quencies $\omega_1, \omega_2, \omega_3$ ($\omega_1 = \omega_2 + \omega_3$) and with envelopes of electric field written in the form

$$E^{(l)}(x,z,t) = \tag{1}$$

$$\frac{1}{2}\left\{ E^{(l)}(x,z)\, \exp(\mathrm{i}(\omega_l t - k_{0l} n_{zl} z)) + \mathrm{c.c.} \right\},$$

where we use $l = 1,2,3$ for pump, signal, and idler waves, respectively, $k_{0l} = \omega_l/c$ are the free space wavenumbers; c is the speed of light in vacuum; $\mathrm{i} = \sqrt{-1}$, and $n_{zl} = n_l \cos\Theta_l$ are the reference indices, Θ_l are tilt angles measured in respect to the propagation direction z. The evolution of these field envelopes can be described by a set of Helmholtz equations with nonlinear propagation operator $\hat{P}^{\mathrm{NL}}_{(l)}$:

$$-\frac{1}{k_{0l}^2 n_{zl}^2}\frac{\partial^2 E^{(l)}}{\partial^2 z} + \frac{2\mathrm{i}}{k_{0l} n_{zl}}\frac{\partial E^{(l)}}{\partial z} = \hat{P}^{\mathrm{NL}}_{(l)} E^{(l)}, \tag{2}$$

$$\hat{P}^{\mathrm{NL}}_{(l)} = \frac{1}{k_{0l}^2 n_{zl}^2}\Big(\frac{\partial^2}{\partial^2 x} + k_{0l}^2\big(n_l^2(x,z) - n_{zl}^2\big)\Big) + \frac{k_{0l}^2 G^{(l)}(x,z)}{E^{(l)}(x,z)}, \tag{3}$$

where $n_l(x,z)$ are the distributions of indices for each frequency and $G^{(l)}(x,z)$ are nonlinear coupling terms defined by

$$G^{(1)}(x,z) = \chi^{(2)}_m(x)\, E^{(2)}(x,z)\, E^{(3)}(x,z)\, \exp(-\mathrm{i}\Delta\beta_z z),$$

$$G^{(2)}(x,z) = \chi^{(2)}_m(x)\, E^{(1)}(x,z)\, E^{(3)*}(x,z)\, \exp(\mathrm{i}\Delta\beta_z z), \tag{4}$$

$$G^{(3)}(x,z) = \chi^{(2)}_m(x)\, E^{(1)}(x,z)\, E^{(2)*}(x,z)\, \exp(\mathrm{i}\Delta\beta_z z),$$

where $\chi^{(2)}_m(x)$ are Fourier coefficients of nonlinear susceptibility modulated with period Λ of sign reversal [15] for quasi-phase matching (QPM) of three wave mixing in the mth diffraction order in PPLN material, $\Delta\beta_z$ is phase matching condition projection on propagation direction z of field envelopes. For tilted propagation of three waves at Θ_l angle we have $\Delta\beta_z = k_{02}n_{z2} + k_{03}n_{z3} - k_{01}n_{z1} + g_z m$, where g_z is projection of modulus of nonlinear grating wavevector $|\mathbf{g}| = 2\pi/\Lambda$ on propagation direction z. SVEA approximation can be obtained from Eq. (2) by neglecting the $|\partial^2 E^{(l)}/\partial^2 z|$ term with respect to $|2\mathrm{i}k_{0l}n_{0l}|\partial E^{(l)}/\partial z$ and getting the set of Fresnel equations which can be solved by the simple paraxial finite-difference BPM [3, 4] (FD-BPM).

As suggested for nonparaxial equations in [11] and for single linear Helmholtz equation in [4, 16], we can derive Padé approximants of Eq. (2) through some recurrence relations and write these equations in a useful propagator form

$$\frac{\partial E^{(l)}}{\partial z} = -\mathrm{i}k_{0l} n_{zl}\frac{\hat{N}^{(l)}}{\hat{D}^{(l)}} E^{(l)}, \tag{5}$$

where the expressions of the $\hat{N}^{(l)}$, $\hat{D}^{(l)}$ operators for the Padé $(1,1)$ approximant are

$$\hat{N}^{(l)} = \frac{\hat{P}^{\mathrm{NL}}_{(l)}}{2}, \qquad \hat{D}^{(l)} = 1 + \frac{\hat{P}^{\mathrm{NL}}_{(l)}}{4}. \tag{6}$$

The finite-difference equations may be derived from Eqs. (5) by introducing a discretization lattice $x = i\Delta x$, $z = p\Delta z$ for electric field envelopes $E^{(l)}_{i,p}$, applying the implicit quasi-Crank–Nicholson finite-difference approximation of derivative [3, 4] in the direction of propagation z, using central finite-difference approximation of the derivatives in the transverse x direction, and evaluating nonlinear coupling terms in the previous propagation layer,

$$\hat{D}^{(l)}\frac{E^{(l)}_{i,p+1} - E^{(l)}_{i,p}}{\Delta z} = \tag{7}$$

$$-\mathrm{i}\hat{N}^{(l)}\big[\alpha E^{(l)}_{i,p+1} - (1-\alpha)E^{(l)}_{i,p}\big],$$

which form a tridiagonal linear system of equations and can be solved by the Thomas algorithm, where α is quasi-Crank–Nicholson parameter [13].

To simulate open space propagation in finite size computation domain, the proper nonreflecting boundary conditions should be applied at the upper and lower boundaries of computation domain to remove spurious wave reflections from boundaries that dramatically degrade the quality of results. The oldest method to introduce absorbing boundary conditions (ABC) in BPM is to put medium with complex refraction index $n_l(x,z) = \mathrm{Re}\, n_l(x,z) + \mathrm{i}\,\mathrm{Im}\, n_l(x,z)$ at boundaries [17]. But this method is numerically very expensive because it requests a large number of grid points at boundaries and careful optimization of complex index profiles.

The most popular and efficient method for paraxial simulation is to use transparent boundary conditions (TBC) where field at boundary is approximated

by plane wave with the value guessed from the known field on the previous propagation z-step [5],

$$E^{(l)}(x_0)/E^{(l)}(x_1) = \beta_l \exp(\mathrm{i}k_{xl}\Delta x)\,, \qquad (8)$$

and a sign of k_{xl} is checked to ensure only radiation outflow. In this work we will test performance of three realizations of TBC for nonparaxial BPM. In the first formulation, adaptive TBC, no restrictions on β_l were applied. In the second one, controlled TBC, the value of β_l was checked and for cases of $\beta_l > 1$ the substitution $\beta_l = 1$ was used. In the third one, uniform TBC, for all cases $\beta_l = 1$ was used, which corresponded to uniform single plane wave approximation at the boundary of computation domain.

The third method to introduce efficient nonreflecting boundaries is to use PML boundary conditions [7, 8]. Contrary to the first case of ABC, PML is an artificial absorbing material layer placed at the boundaries [10]. The idea is not to use a physical absorber with complex refraction index, but to change the propagation equations by introducing anisotropic conductivities $\sigma_{xl}(x)$ for x coordinate in PML media and by performing complex anisotropic mapping of Eqs. (3). In this media we will use and test the nonlinear propagation operators $\hat{P}_{(l)}^{\mathrm{NL-PML}}$ for $\chi^{(2)}$ nonlinear PML (NL-PML) media written as

$$\hat{P}_{(l)}^{\mathrm{NL-PML}} = \frac{1}{k_{0l}^2 n_{zl}^2}\Big(\frac{1}{1-\mathrm{i}\mu_l\sigma_{xl}(x)}\frac{\partial}{\partial x}\Big[\frac{1}{1-\mathrm{i}\mu_l\sigma_{xl}(x)}\frac{\partial}{\partial x}\Big] + k_{0l}^2(n_{pl}^2 - n_{zl}^2) + k_{0l}^2\frac{G^{(l)}(x,z)}{E^{(l)}(x,z)}\Big)\,, \qquad (9)$$

where $\mu_l = \eta_0/k_0 n_{pl}^2$, η_0 is vacuum impedance, n_{pl} are constant refractive indices of NL-PML media for pump, signal, and idler waves, which can be chosen to be equal to the index of the $\chi^{(2)}$ media adjacent to the nonlinear perfectly matched layer. Further, we will also test termination of NL-PML by Dirichlet boundary conditions, $E^{(l)}(x_0) = 0$ (NL-PML-D), and by TBC (NL-PML-TBC).

3. Numerical results

In our test simulations of boundary conditions for open space nonlinear nonparaxial propagation all three interacting beams were extraordinary waves with wavelengths $\lambda_1 = 0.8$ μm, $\lambda_2 = 1.55$ μm, $\lambda_3 = 1.653$ μm, respectively, for pump, signal, and idler waves. We studied the first order QPM interaction of these extraordinary waves through the diagonal nonlinear coefficient of $LiNbO_3$ $d_{33} = 36$ pm/V ($\chi_{33}^{(2)} = 2d_{33}$) [18]. From Sellmeier equations [12] we defined refraction indices of bulk $LiNbO_3$ for three interacting waves as follows: $n_1 = 2.175$, $n_2 = 2.137$, $n_3 = 2.134$. Reference indices in Eqs. (2, 3) were equal to those of bulk $LiNbO_3$, $n_{z1} = n_1$, $n_{z2} = n_2$, $n_{z3} = n_3$ at the relevant frequencies as for non-tilted propagation. BPM treats the propagation of optical field along z as an initial value problem. We launched collineary Gaussian pump and signal beams having half-waists $w_1 = w_2 = 2.828$ μm, and no initial beam for idler was considered. Spatial solitons were excited by pump and signal waves at powers $P_1(0) = 8{\cdot}10^{10}$ W/m and $P_2(0) = 8{\cdot}10^{7}$ W/m, respectively, and with phase mismatch $\Delta\beta = 97.6$ m^{-1} produced by $\chi^{(2)}$ grating with period $\Lambda = 20.316$ μm and duty cycle 0.5.

It is defined [14] that the paraxial FD-BPM model can be used up to 15° tilt, and nonparaxial BPM based on Padé (1, 1) approximants (Eqs. (5)) – up to 30° tilt beam propagation. Therefore we investigated the effectiveness of boundary conditions for nonparaxial propagation at 5° and 30° tilted propagation. In the PML medium, we assumed a distribution of conductivities for pump, signal, and idler waves as $\sigma_{x1}(\rho) = \sigma_{x2}(\rho) = \sigma_{x3}(\rho) = \sigma_m(\rho/\delta)^N$, where σ_m is the maximum conductivity, δ is the PML layer thickness, N is the order of the polynomial used for conductivity profile function, ρ is the distance from the beginning of the PML. For both angles of test beam propagation the thickness of the PML layer is $\delta = 0.8$ μm, polynomial order $N = 2$, and width of computation window 20 μm including two PML layers. For 5° tilt, discretization is $\Delta x = \Delta z = 0.04$ μm and computation window length is 300 μm. For 30°, $\Delta x = 0.03$ μm, $\Delta z = 0.02$ μm, and window length is 50 μm. At these propagation distances spatial solitary waves experience a single reflection from boundary. To quantitatively assess the effectiveness of boundary conditions we study the global integral errors defined as follows:

$$\varepsilon_{\mathrm{integ}}^{(l)} = \frac{\sum_z \sum_x \left|I_{\mathrm{comp}}^{(l)}(x,z) - I_{\mathrm{exact}}^{(l)}(x,z)\right|^2}{\sum_z \sum_x \left|I_{\mathrm{exact}}^{(l)}(x,z)\right|^2}\,, \qquad (10)$$

where $I_{\mathrm{comp}}^{(l)}(x,z)$ are computed intensities of optical fields, $I_{\mathrm{exact}}^{(l)}(x,z)$ are reference intensities of optical field defined as exact, i. e. without soliton reflection from the boundary and computed by the nonparaxial method for the computation window width 160 μm.

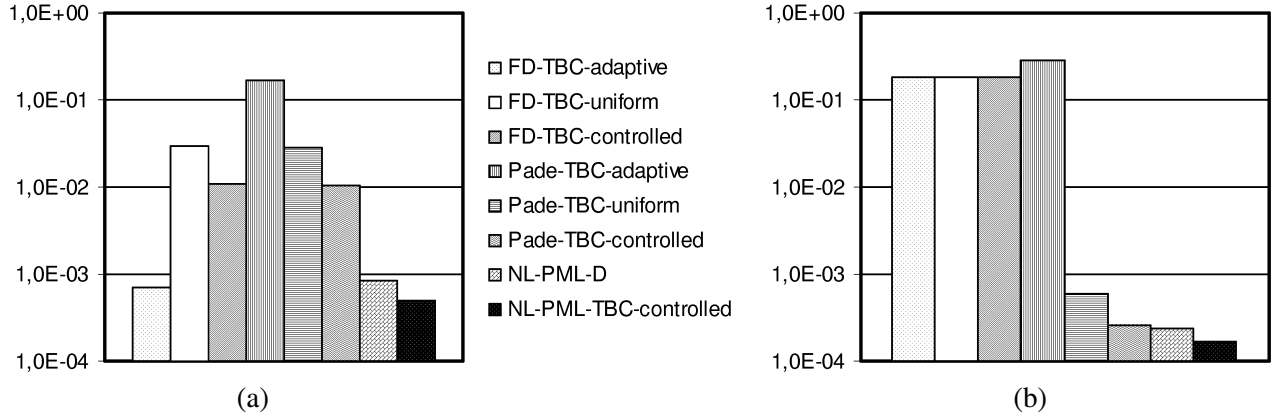


Fig. 1. Integral global errors (y axis) for various formulations of boundary conditions for paraxial (FD-adaptive, uniform, and controlled TBC) and nonparaxial (Padé-adaptive, uniform, and controlled TBC and NL-PML) propagation of pump wave component of spatial soliton at the (a) 5° and (b) 30° tilt angles.

While performing evaluation of $\varepsilon^{(l)}_{\text{integ}}$ the mesh points of PML media are not included.

NL-PML media can be terminated by Dirichlet boundary conditions (PML-D), i. e. the field at the boundary mesh point is evaluated by $E^{(l)}(x_0) \equiv 0$, or by TBC. If $R^{\text{TBC/D}}$ is a reflection coefficient of the PML layer outer limit, terminated by TBC or Dirichlet boundary conditions, respectively, then for Dirichlet boundary conditions $R^{\text{D}} = 1$ and for TBC $R^{\text{TBC}} \ll 1$. Thus, one could usually expect smaller reflectivity for termination of PML media by TBC. This above statement about TBC reflectivity is working properly only for paraxial FD-BPM simulation (see Fig. 1(a, b)). In contrast, the nonparaxial formulation using Padé approximants of the propagation operator permits superposed waves with very different k_{xl} values, and the single plane wave approximation at boundary then becomes very poor [4]. It is well known [9] that TBC fails for highly diverging beam and for the cases of interference at boundary of multiple outgoing plane waves. Figure 1 shows the global integral errors for pump wave component of spatial soliton induced by reflection from boundary versus soliton propagation angle and formulation of boundary conditions. For paraxial FD-BPM the adaptive TBC shows the best performance. Big $\varepsilon^{(l)}_{\text{integ}}$ of all formulations of FD-TBC for 30° tilt angle is mainly caused not by boundary conditions but by failure in the direction of propagation of spatial soliton simulated by paraxial FD-BPM. On the contrary, for nonparaxial numerical technique based on Padé (1, 1) approximant, adaptive TBC demonstrate the worst performance both for 5° and 30° tilt angles. Uniform and controlled TBC give comparable performance for paraxial as well as nonparaxial propagation at the 5° tilt angle. The controlled TBC show better results than uniform TBC. Figure 1 also includes results on $\varepsilon^{(l)}_{\text{integ}}$ for NL-PML boundary conditions terminated by Dirichlet boundary conditions and controlled TBC applied in the nonparaxial numerical technique. Simulations were performed for NL-PML-TBC with $\sigma_m = 2{\cdot}10^5$ $(\Omega{\cdot}\text{m})^{-1}$ and $\sigma_m = 2{\cdot}10^4$ $(\Omega{\cdot}\text{m})^{-1}$ for 5° and 30° tilt angles, respectively. For NL-PML-D we used $\sigma_m = 4{\cdot}10^5$ $(\Omega{\cdot}\text{m})^{-1}$ and $\sigma_m = 10^5$ $(\Omega{\cdot}\text{m})^{-1}$ for 5° and 30° tilt angles, respectively. It is clear that NL-PML together with controlled TBC give the best results.

Further improvement of this performance can be obtained by optimizing values of PML layer parameters N, σ_m, and δ. Figure 2 presents dependence of integral global errors of boundary conditions on conductivity profile polynomial order N. It is clear that optimal performance for average 5° and 30° tilted beam propagation is $N = 2$. Figure 2 also shows effect of nonlinearity on performance of PML. Due to better index matching at boundaries in nonlinear interaction regime the NL-PML has lower reflectivity, especially at 5° tilt angles, than linear PML (L-PML). To achieve lowest reflectivity from boundaries of computation domain, it is important to correctly choose σ_m and δ parameters of PML. Figure 3 depicts results of optimization of these PML parameters. It is shown that the NL-PML terminated by controlled TBC usually have better performance than NL-PML terminated by Dirichlet boundary conditions. There is an optimal σ_m to obtain minimal $\varepsilon^{(l)}_{\text{integ}}$. In Fig. 1(a) we can see some instability of NL-PML terminated by controlled TBC. But by increasing the PML thickness δ (Fig. 3(b)), this instable behaviour disappears and we can reduce errors almost by two orders for NL-PML-controlled-TBC as compared to NL-

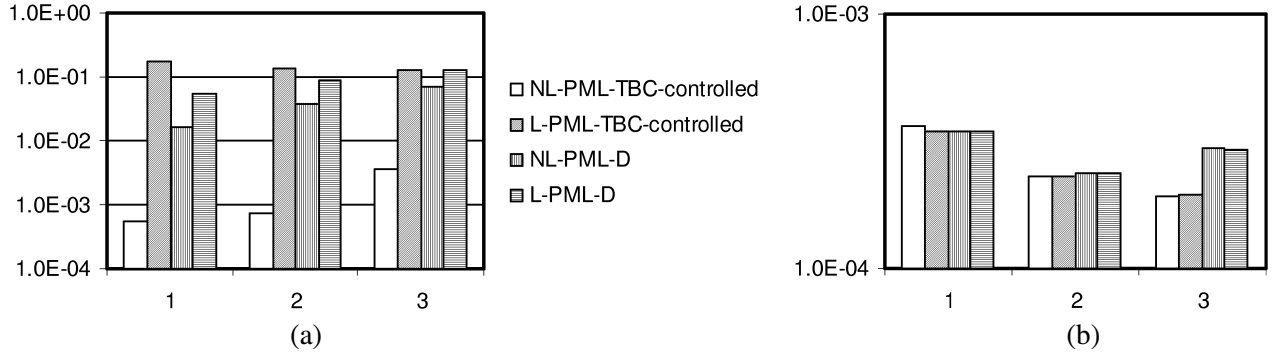


Fig. 2. Integral global errors (y axis) versus conductivity profile polynomial order N for linear and nonlinear PML boundary conditions for nonparaxial propagation of pump wave of parametric spatial soliton at the (a) 5° and (b) 30° tilt angles.

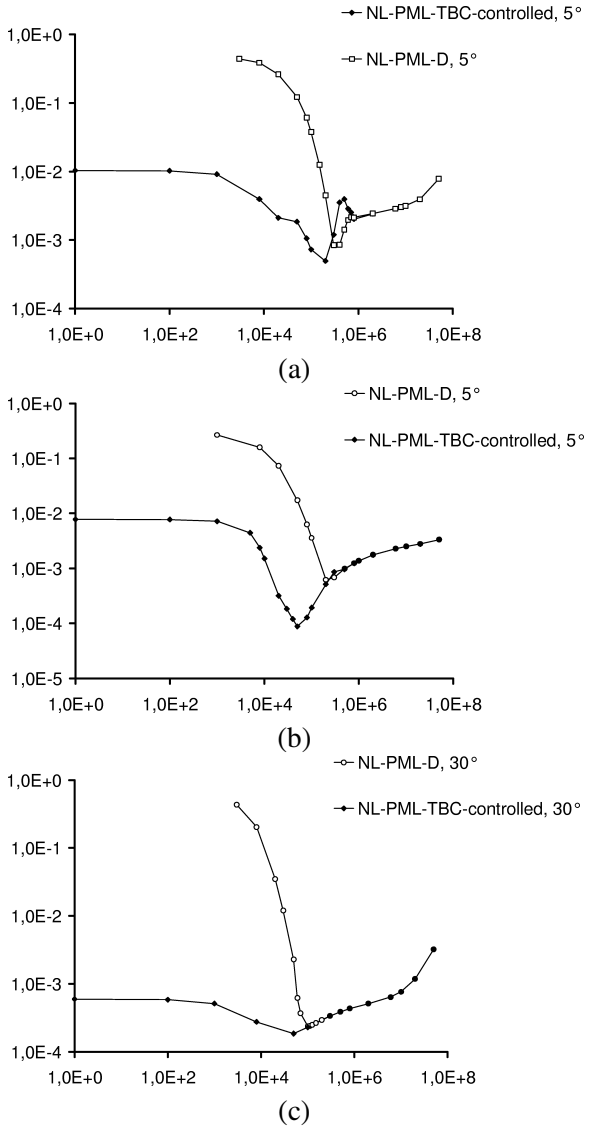


Fig. 3. Integral global errors (y axis) versus maximum conductivity σ_m ($[\Omega{\cdot}\mathrm{m}]^{-1}$, x axis) for (a) 5° tilt angle and 0.8 μm PML layer thickness, (b) 5° tilt angle and 1.6 μm PML layer thickness, (c) 30° tilt angle and 0.8 μm PML layer thickness, NL-PML terminated by Dirichlet boundary conditions and controlled TBC.

PML-D. This effect of decreasing of boundary reflectivity is more visible for small angle tilted soliton propagation. For 30° tilted propagation of spatial soliton, (Fig. 3(c)), the difference between minima of $\varepsilon_{\mathrm{integ}}^{(l)}$ is much smaller. NL-PML-D boundary conditions have higher reflectivity than NL-PML-controlled-TBC, but the advantage of termination of NL-PML by Dirichlet boundary conditions is higher stability and robustness of these boundary conditions.

4. Conclusion

In this work testing of different formulations of boundary conditions for paraxial and nonparaxial FD-BPM was carried out. It is defined that adaptive TBC formulation is the best one for paraxial beam propagation but the worst one for the nonparaxial beam propagation method. Introduction of controlled TBC yields better performance than adaptive TBC for nonparaxial BPM. The NL-PML is more efficient than linear PML boundary conditions for small tilt angle nonparaxial beam propagation, because it reduces index mismatching at boundaries induced by optical nonlinearity. This effect is important at small tilt angle propagation of spatial solitons. It is established that NL-PML terminated by Dirichlet boundary conditions is more robust. The NL-PML terminated by controlled TBC gives the best performance for small tilt angle nonparaxial propagation providing optimization of NL-PML thickness and maximum conductivity.

Acknowledgements

This research was partially supported by the Lithuanian State Science and Studies Foundation grants COST P8, Reg. No. V-04033 and MODELITA, Reg. No. C-

03048. The author is grateful to Prof. Paolo Bassi and Dr. Gaetano Bellanca for many helpful discussions.

References

[1] A. Taflove and S.C. Hagness, *Computational Electrodynamics: The Finite-Difference Time-Domain Method*, 2nd ed. (Artech House, Norwood, 2000).

[2] N.-N. Feng and W.-P. Huang, A field-based numerical method for three-dimensional analysis of optical waveguide discontinuities, IEEE J. Quantum Electron. **39**, 1661–1665 (2003).

[3] H.J.W.M. Hoekstra, On beam propagation methods for modelling in integrated optics, Opt. Quantum Electron. **29**, 157–171 (1997).

[4] R. Scarmozzino, A. Gopinath, R. Pregla, and S. Helfert, Numerical techniques for modelling guided-wave photonic devices, IEEE J. Select. Top. Quantum Electron. **6**, 150–162 (2000).

[5] G.R. Hadley, Transparent boundary conditions for beam propagation methods, Opt. Lett. **16**, 624–626 (1991).

[6] F. Ma, C.L. Xu, and W.P. Huang, Wide-angle full vectorial beam propagation method, IEEE Proc. - Optoelectron. **143**, 139–143 (1996).

[7] J.P. Bérenger, A perfectly matched layer for the absorption of electromagnetic waves, J. Comput. Phys. **114**, 185–200 (1994).

[8] C.M. Rappaport, Perfectly matched absorbing boundary conditions based on anisotropic lossy mapping of space, IEEE Microwave Guided Wave Lett. **5**, 90–92 (1995).

[9] C. Vassallo and F. Collino, Highly efficient absorbing boundary conditions for beam propagation method, J. Lightwave Technol. **14**, 1570–1577 (1996).

[10] W.P. Huang, C.L. Xu, W. Lui, and K. Yokoyama, The perfectly matched layer (PML) boundary condition for the beam propagation method, IEEE Photon. Technol. Lett. **8**, 649–651 (1996).

[11] R. Petruskevicius, G. Bellanca, and P. Bassi, Nonlinear PML boundary conditions for nonparaxial BPM in $\chi^{(2)}$ materials, IEEE Photon. Technol. Lett. **10**, 1434–1436 (1998).

[12] L.E. Myers, R.C. Eckardt, M.M. Fejer, R.L. Byer, W.R. Bosenberg, and J.W. Pierce, Quasi-phase-matched optical parametric oscillators in bulk periodically poled $LiNbO_3$, J. Opt. Soc. Am. B **12**, 2102–2116 (1995).

[13] R. Petruškevičius, G. Bellanca, and P. Bassi, BPM modelling of three-wave interaction in periodically poled second-order nonlinear materials, Lithuanian J. Phys. **38**, 168–176 (1998).

[14] R. Petruskevicius, Modelling of nonparaxial propagation of parametric spatial solitons, Proc. SPIE **4415**, 231–236 (2001).

[15] P. Baldi, P. Aschieri, S. Nouh, M. de Micheli, D.B. Ostrowsky, D. Delacourt, and M. Papuchon, Modelling and experimental observation of parametric fluorescence in periodically poled lithium niobate waveguides, IEEE J. Quantum Electron. **31**, 997–1008 (1995).

[16] G.R. Hadley, Wide-angle beam propagation using Padé approximant operators, Opt. Lett. **17**, 1426–1428 (1992).

[17] M.D. Feit and J.A. Fleck, Light propagation in graded-index optical fibers, Appl. Opt. **17**, 3990–3998 (1978).

[18] G.I. Stegeman, D.J. Hagan, and L. Torner, $\chi^{(2)}$ cascading phenomena and their applications to all-optical signal processing, mode-locking, pulse compression and solitons, Opt. Quantum Electron. **28**, 1692–1740 (1996).

EFEKTYVIŲ NETIESINIŲ TOBULAI SUDERINTŲ SLUOKSNIŲ KRAŠTINIŲ SĄLYGŲ MODELIAVIMAS NEGRETAAŠIAM PLUOŠTO SKLIDIMO METODUI

R. Petruškevičius

Fizikos institutas, Vilnius, Lietuva

Santrauka

Netiesinės tobulai suderintų sluoksnių kraštinės sąlygos sėkmingai pritaikytos negretaašiam pluošto sklidimo metodui. Parodyta, kad netiesiniai tobulai suderinti sluoksniai ypač veiksmingai sugeria erdvinius solitonus, krintančius į skaičiavimo srities kraštą, esant plačiam kampiniam bangų sklidimo spektrui. Naudojant pakankamai glotnius laidumo profilius ir netiesinių tobulai suderintų sluoksnių užbaigimą kontroliuojamomis skaidriomis kraštinėmis sąlygomis, galima papildomai žymiai pagerinti skaitmeninių sprendinių tikslumą, nagrinėjant negretaašių pluoštų sklidimą mažais kampais.